

High initial-time sensitivity of medium-range forecasting observed for a stratospheric sudden warming

Yuhji Kuroda¹

Received 27 May 2010; revised 8 July 2010; accepted 12 July 2010; published 20 August 2010.

[1] High initial-time sensitivity for the predictable period of the tropospheric Northern Annular Mode (NAM) around the stratospheric sudden warming (SSW) in the winter of 2003–4 is examined using ensemble simulations of a general circulation model. It is found that the predictable period tends to become very long and reaches to a few months when a forecast is performed before the occurrence of the SSW. When the initial time is set after the SSW, however, the predictable period turns out to be very short. As a result, the predictable limit of time tends to become far longer when forecasts are performed before the occurrence of the SSW compared with those performed after. Comparison is made with winter of 2005–6 with a major SSW and prominent stratospheric variability. The reason for the appearance of such high initial-time sensitivity is discussed. **Citation:** Kuroda, Y. (2010), High initial-time sensitivity of medium-range forecasting observed for a stratospheric sudden warming, *Geophys. Res. Lett.*, 37, L16804, doi:10.1029/2010GL044119.

1. Introduction

[2] Weather forecasting is an important basic technology for general society. Although short-term forecasting is now considered to be relatively reliable, forecasting beyond a few weeks is difficult due to the chaotic nature of atmospheric dynamics [Lorenz, 1963]. However, recent studies of medium-range forecasting have shown that slowly varying lower boundary conditions such as sea surface temperature (SST) and soil moisture can be used as predictors for medium-range forecasting [e.g., Kanamitsu *et al.*, 2002].

[3] Recent advanced studies have shown that stratospheric conditions can be used as an additional predictor of tropospheric variability [Christiansen, 2005; Kuroda, 2008a, hereafter K08]. In particular, Christiansen [2005] showed that inclusion of variability of the stratospheric Northern Annular Mode (NAM) [Thompson and Wallace, 1998; Baldwin and Dunkerton, 2001] significantly improves tropospheric weather forecasts by analyses of observation and model simulations. K08 also showed the importance of the stratosphere by comparing models with and without the stratosphere included. He also found that the predictable period of the NAM variability in the troposphere is very large and reaches to almost two months if the forecast is initialized from shortly before the occurrence of the stratospheric

sudden warming (SSW) of January 2004. Note that this winter was characterized by prominent low-frequency variability in the stratosphere, called the Polar-night Jet Oscillation (PJO) [Kuroda and Kadera, 2001].

[4] Thus, it is interesting to see how the predictable period changes when changing the initial time of the forecast, and how the stratospheric condition is related to such changes. We address this problem by analyzing a set of ensemble forecasts throughout the winter of 2003–4.

[5] This paper is organized as follows. Section 2 describes the data and principal method of analysis. After the presentation of the results in Section 3, Section 4 offers discussion and remarks.

2. Model and Method of Analysis

[6] The numerical model and the method of analysis are the same as were used by K08. The model used is the general circulation model (GCM) developed with the cooperation of the Japan Meteorological Agency (JMA) and the Meteorological Research Institute (MRI) of Japan for seasonal forecasting [Mizuta *et al.*, 2006]. The model is triangularly truncated at a total wave number of 95 (~200-km grid) and with a 40-layer hybrid pressure-sigma coordinate system with an upper boundary at 0.4 hPa (~55-km height). Initial conditions are taken from the objective analysis data produced by JMA, and the data are first modified according to the non-linear normal mode initialization method to remove the initial shock from the fast gravity wave. Land processes are included in the model, and their initial values are also obtained from JMA analyses. For the sea surface temperature (SST), it is assumed that the analyzed anomalous SST at the initial time persists throughout the simulation period, although in reality the SST varies with the seasonal cycle.

[7] Numerical forecasts are performed every 6 hours from the objective analysis data. Predictability is then estimated for every day from recent 5-day data that comprising 20 runs. Thus, the present ensemble forecast is substantially the Lagged Averaged Forecasting (LAF) Method. Predictability is evaluated using the Student's-*t* statistics of anomalous zonal winds of ensemble runs.

[8] We use the anomalous zonal wind at around 60°N (averaged from 55 to 65°N) as a simple index of the NAM [Thompson and Wallace, 1998; Baldwin and Dunkerton, 2001] for the observations and the forecasts.

[9] The referenced observational data we used are the reanalysis data of the National Center of Environmental Forecast (NCEP)/National Center of Atmospheric Research (NCAR) [Kistler *et al.*, 2001]. Daily climatological data are created from these data for the period 1958 to 2001, and then the anomalous wind is defined as the departure

¹Meteorological Research Institute, Tsukuba, Japan.

from daily climatology both for the observations and model results.

3. Results

[10] In the winter of 2003–4, a major stratospheric sudden warming (SSW) took place with a peak temperature of 235 K for the polar cap (averaged poleward of 80°N) and a peak easterly zonal wind of 11 m/s at around 60°N at 10 hPa on 9 January 2004, and a very prominent PJO-type variability appeared (Figure 1 of K08). This variability should play a key role in making better predictions of the tropospheric NAM variability as was shown by K08. Figure 1 compares the time evolution of the anomalous zonal-mean zonal winds around 60°N for the observation (Figure 1a) and the forecasts (Figures 1b–1d). Figure 1b (Figure 1c) shows the forecast calculated from an ensemble of 06Z 27 December 2003 to 00Z 1 January 2004 (06Z 10 January to 00Z 15 January 2004). We shall hereafter call the former forecast F1 and the latter F2. Shading indicates the statistical significance as evaluated by the Student's *t* statistics of each ensemble.

[11] When a forecast is performed before the occurrence of the SSW, as in F1, the weaker zonal wind associated with the SSW at the beginning stage in the stratosphere and the following slow propagation to the lower stratosphere is relatively well captured by the simulation, although temporally shorter variabilities in the observation are not well simulated. It would be interesting to show that a statistically significant negative tropospheric NAM for about two months could be predicted. It would also be interesting to observe that NAM variabilities in the troposphere are created at the same time in the troposphere when the signal appears in the lower stratosphere. This should correspond to the fact that the tropospheric NAM signal is almost instantaneously controlled through the meridional circulation driven by momentum forcings in the lower stratosphere [Kuroda and Kodera, 2004]. Thus, a stronger tropospheric NAM signal should correspond closely to a stronger signal in the lower stratosphere. It should be noted that the tropospheric NAM signal is especially statistically stronger around 25 January, 20 February, and 1 March, which roughly correspond to the signals in the observation. This suggests that if stratospheric variabilities can be well simulated in the model, tropospheric NAM signals can also be well simulated. However, the tropospheric NAM signal is statistically weaker than that of the stratosphere.

[12] When a forecast is performed after the occurrence of the SSW, as in F2, it is found that the downward propagating NAM signal in the stratosphere weakens. However, it remains significant in the lower stratosphere until early March. Consistent with the weaker stratospheric signal, a statistically significant tropospheric NAM signal lasts only about a half a month after the forecast. Note that the higher statistical significance of the forecasts for the first week originate from the initial conditions.

[13] Figures 1b and 1c compare two typical examples of forecasts with initial times before and after the SSW. To see the overall changes in the predictability of the tropospheric NAM with changes in the initial time around the SSW, Figure 1d shows forecasts at the 850-hPa level as a function of the initial time. It can be seen that the predictable period is almost until the beginning of March regardless of the initial time when the forecast is performed before the occurrence of

the SSW. Therefore, the predictable period is longer if the forecast is performed earlier, but the statistical significance tends to be weaker. On the other hand, the predictable time reduces to only about a half a month if the forecast is performed after the SSW. Thus, the predictable time is drastically changed by changing the initial time around the SSW.

[14] To study the differences between forecasts F1 and F2 in more detail, we compare the time evolutions of the daily anomalous zonal-mean zonal wind and Eliassen–Palm (E–P) flux (Figure 2). For both forecasts F1 (Figure 2b) and F2 (Figure 2c), although the simulation is very similar to the observation both for the zonal wind and the E–P flux for the beginning of forecasts, the agreement becomes worse over time. However, comparison of these two forecasts shows that the forecast of the zonal wind of F1 is better than that of F2 for 29 January and after. In fact, if pattern correlations of the zonal winds are calculated, those of F1 drop to 0.8 on 15 January, but maintain a value of around 0.8 until the middle of February. In contrast, those of F2 drop nearly linearly with time, and then those after February tend to have smaller values than those of F1 (not shown). Compared with the zonal wind, the similarity of the E–P flux is limited in the upper levels both for F1 and F2 after 2 weeks of forecasts. The result suggests better forecasts depend on how well wave-mean flow interactions are simulated in the stratosphere. In fact, if F1 and F2 are compared, the amplitude of the stratospheric winds is better reproduced for F1 than for F2 after 29 January. Such accurate representation of the stratosphere will create well-reproduced NAM variability in the troposphere through dynamical coupling. Thus, the difference between these forecasts likely originates from better forecasts of the stratosphere for F1 compared with F2.

[15] The predictable periods of tropospheric NAM are very different between forecasts F1 and F2. Therefore, we compare the time evolution of the anomalous zonal-mean zonal wind around 60°N for F1 and F2 (Figure 3). From the simulation of F1 it can be seen that the ensemble mean does not necessarily capture very well the observed variability of the zonal wind after about 8 January. However, it has some similarity with the low frequency variability of the observation. What is interesting is that most of the ensemble members forecast significant negative values for late January and after. In comparison, for the simulation of F2 the ensemble mean captures the observed features well only until about 20 January. For the time evolution after late January, each member spreads widely around the zero line and the ensemble mean cannot be regarded as significantly negative. This is why F1 forecasts significant negative tropospheric NAM but F2 does not. The difference between these two should originate from different strengths of the NAM signals in the lower stratosphere. In fact, F1 forecasts a larger temperature anomaly, which should produce a larger negative NAM response in the troposphere, as shown by Haigh *et al.* [2005].

4. Discussion and Remarks

[16] High initial-time sensitivity of medium-range forecasting for initial times around the SSW of January 2004 is observed. Very long tropospheric NAM predictable periods of up to a few months are found if the forecast is performed before the occurrence of the SSW, but the periods are limited to only half a month if it is performed after the SSW (Figure 1d).

[17] Figure 1 also shows that regardless of the initial time of the forecast, a higher significant area appears for some specific periods (e.g., 1, 10, 20 February, and 1 March) if the forecast is performed before the SSW. These correspond with the appearance of stronger signals in the lower stratosphere that do not depend on the initial time of forecast. It is also

interesting to note that regardless of the initial time of the forecast, NAM signals turn positive around 15 March. Note that this period corresponds to a phase change of the PJO (from anomalous easterly to westerly wind in the stratosphere). This means that the model captures well the slower time evolution of the PJO regardless of the initial time.

[18] We found the high initial-time sensitivity to be a property of the forecast with the SSW of January 2004. It is a question whether such high initial-time sensitivity will always appear with the SSW when a prominent PJO-type variability appears in the stratosphere. Therefore, we performed one more experiment in a winter when a PJO-type variability appeared; we selected the winter of 2005–6. A major SSW with a peak temperature of 250 K for the polar cap appeared on 22 January with a peak easterly zonal wind of 20 m/s around 60°N at 10 hPa on 26 January 2006. A PJO-type variability was also very prominent, and the SST in the northern Atlantic Ocean was anomalously higher, similar to the winter of 2003–4. Figure 4 is the same as Figure 1 except for the winter of 2006. It can be seen that the downward propagation of the NAM signal to the troposphere until the end of March is very prominent in the observation (Figure 4a). When the forecast is performed before the occurrence of the SSW as in Figure 4b, long-lasting significant negative tropospheric NAM signals is predicted through the end of March, although the statistical significance is weaker than that for those predicted for 2004. On the other hand, when a forecast is performed after the SSW as in Figure 4c, the predictable period is very short. If the predictable period is shown as a function of the initial time (Figure 4d), it can be seen that the predictable period is longer when the initial time is set before the SSW, but it becomes shorter if the initial time is set after the SSW. However, it can also be seen that the signal is weaker and the initial time with a longer predictable period lasts only about 10 days before the SSW in this winter. It is also interesting to note that a higher predictable period first appears only around 18 and 30 March by downward stratospheric signals, but it then spreads to the whole negative NAM period when the initial time increases from day 0 to 10. A similar time evolution of the predictability period also was found in the winter of 2004 (Figure 1d).

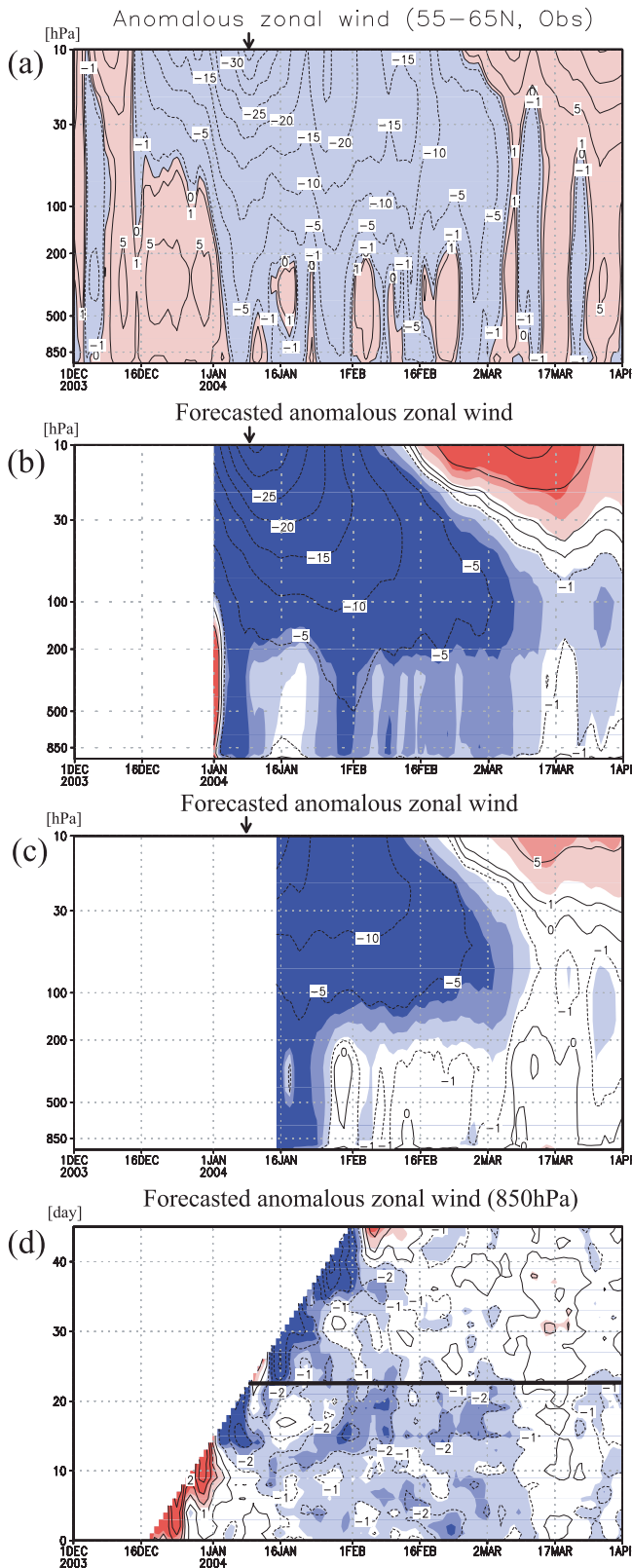


Figure 1. Anomalous zonal wind averaged from 55° to 65°N from 1 December 2003 to 1 April 2004 for (a) NCEP reanalysis and (b–d) forecasts. Figure 1b (Figure 1c) indicates the ensemble mean (contours) of the forecasts and its statistical significance (shading), obtained using initial times between 06Z 27 December 2003 to 00Z 1 January (06Z 10 to 00Z 15 January) 2004. Contours are shown for every 5 m/s from ± 5 m/s and zero, and for ± 1 m/s for Figures 1a–1c, and every 1 m/s for Figure 1d. Dashed lines indicate negative values. In the forecast plot, the shading indicates the statistical significance, with light, middle, and heavy shading indicating 95%, 99.9%, and almost 100% significance (Student's t greater than 2, 4, and 6), respectively. The arrows on the panels indicate the peak day of the observed major SSW. Figure 1d is the same as Figure 1b except for forecasts of the 850-hPa level as a function of 46 continuous initial days from 17 December 2003 to 31 January 2004. The horizontal black line indicates the forecast from the day of maximum stratospheric easterly zonal wind.

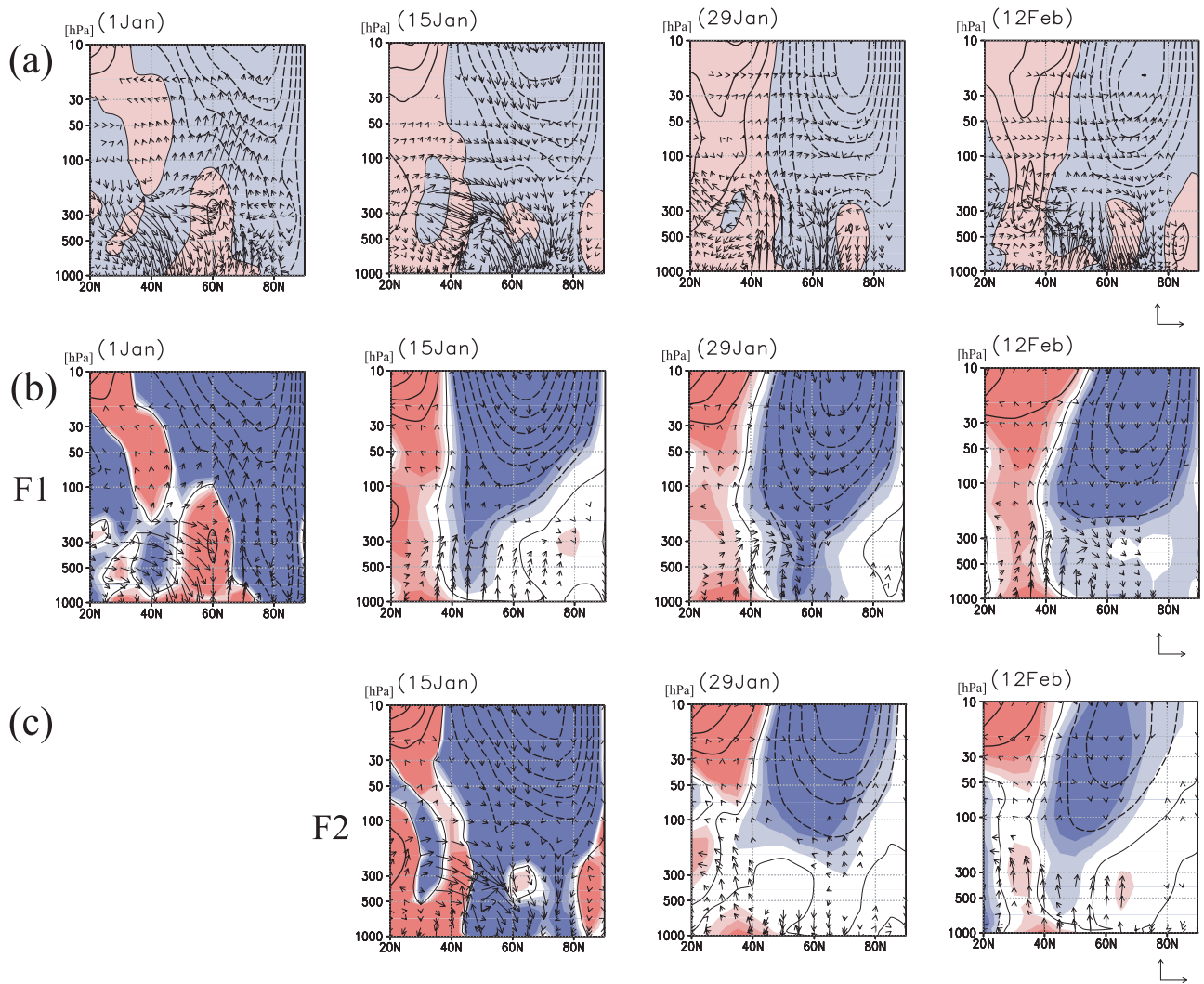


Figure 2. Same as Figure 1 except showing the anomalous zonal-mean zonal wind (contours and shading) and the E-P flux (arrows) for every two weeks of (a) observation and (b and c) forecasts. The E-P flux has been scaled by the reciprocal square root of the pressure, and only arrows that have a statistical significance greater than 95% are shown. The horizontal (vertical) reference arrow indicates $3 \times 10^8 \text{ kg s}^{-2}$ ($1 \times 10^6 \text{ kg s}^{-2}$) on 1000 hPa. Contours are shown for every 5 m/s from $\pm 5 \text{ m/s}$ and zero.

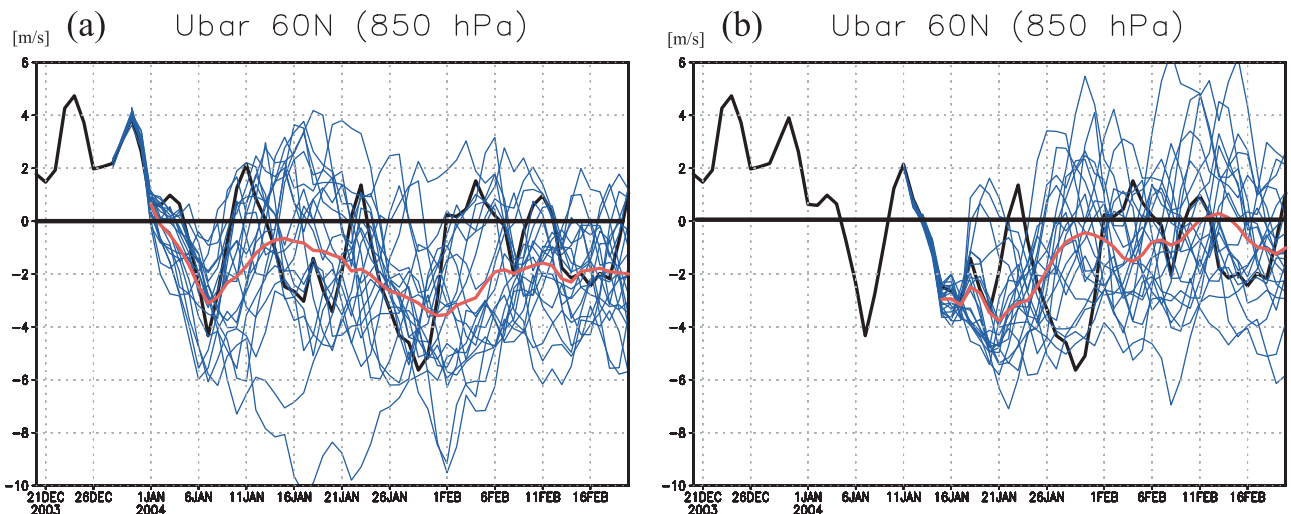


Figure 3. Line plots showing the anomalous zonal-mean zonal wind for (a) F1 and (b) F2. The thick black line indicates the observation. The thin lines indicate each member of the forecasts and the red line is the ensemble mean.

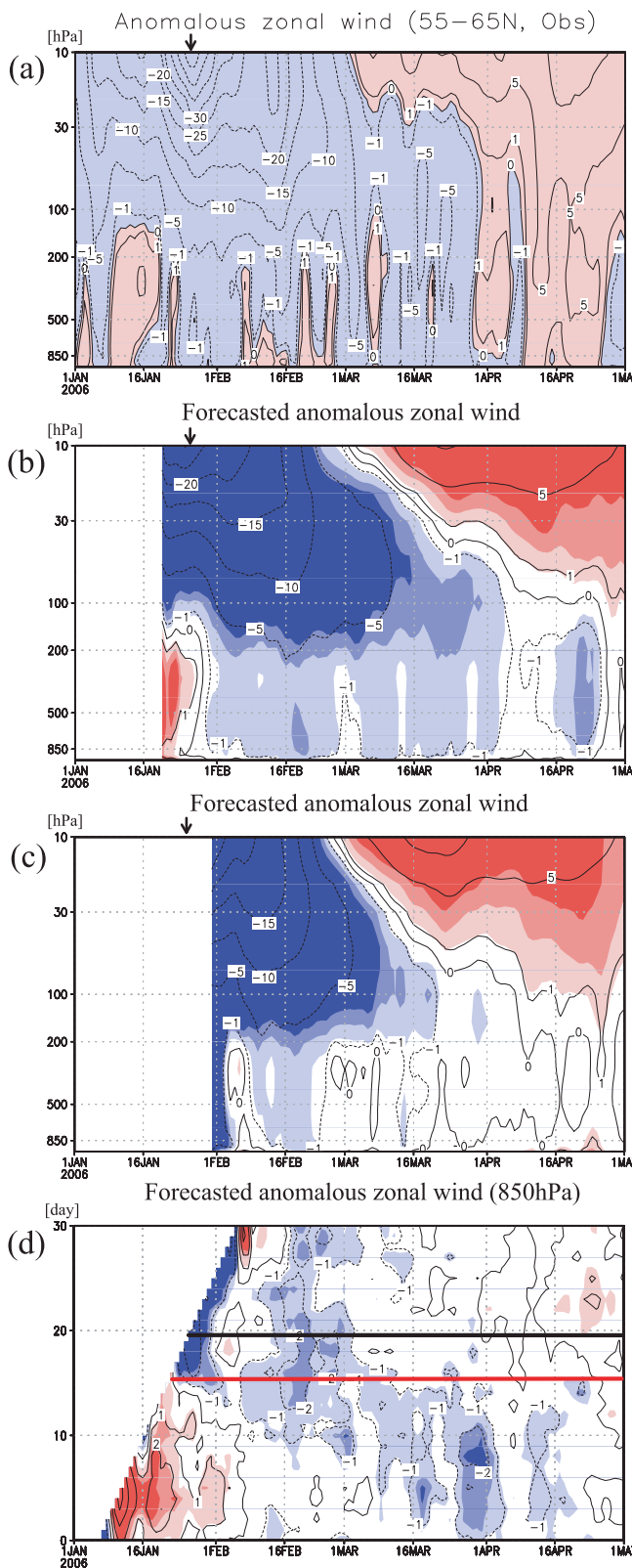


Figure 4. Same as Figure 1 except for (a–d) the period from 1 January to 1 May 2006. Figure 4b (Figure 4c) indicates forecasts using initial times between 06Z 15 to 00Z 20 January (06Z 26 to 00Z 31 January) 2006. Figure 4d indicates 31 initial days from 6 January to 5 February 2006. The horizontal red line indicates the forecast from the day of maximum stratospheric temperature.

[19] The example from 2006 suggests that high initial-time sensitivity exists for any SSW when a prominent PJO appears. However, differences between winters were also found. More examples will be examined in a future study. It should also be noted that the analysis technique used in the present study will tend to overestimate the true predictable period owing to the assumption that the model is perfect.

[20] It would be natural to think that forecasts from later initial times could predict more of the future than those from older initial conditions, because later initial conditions have more future information than older ones. However, the present results contradict this for around the initial time of an SSW. Why does such high initial-time sensitivity appear for an SSW? One possibility comes from the prominent difference in initial conditions between those before and after an SSW. In fact, the initial conditions would include large-amplitude upward-propagating planetary waves if it were made before the SSW, but it would include only small-amplitude waves if it were made after the SSW [e.g., Kuroda, 2008b]. As a result, the former (latter) creates dynamics (radiation) dominant initial conditions. For the dynamics dominant initial conditions, the initialization process can connect the observed initial conditions realistically to the dynamical evolution of the model. However, for the radiation dominant initial conditions, the time evolution can be much more unstable than for the dynamical perturbation by the initialization, and a greater spread can be created among ensembles. In fact, analysis of ensemble runs shows that the mean vertical component of the E-P flux before SSW is significantly anticorrelated with the 60-day mean tropospheric NAM index after SSW (not shown). More study is needed in the future.

[21] **Acknowledgments.** The author is grateful to H. Yoshimura for providing the numerical model used in the present study. He is also grateful to H. Mukougawa for useful comments. This work was supported in part by a Grant-in-Aid (20340129, 20340131) for Science Research of the Ministry of Education, Culture, Sports, Science, and Technology of Japan.

References

- Baldwin, M. P., and T. J. Dunkerton (2001), Stratospheric harbingers of anomalous weather regimes, *Science*, *294*, 581–584, doi:10.1126/science.1063315.
- Christiansen, B. (2005), Downward propagation and statistical forecast of the near-surface weather, *J. Geophys. Res.*, *110*, D14104, doi:10.1029/2004JD005431.
- Haigh, J. D., M. Blackburn, and R. Day (2005), The response of tropospheric circulation to perturbations in lower-stratospheric temperature, *J. Clim.*, *18*, 3672–3685, doi:10.1175/JCLI3472.1.
- Kanamitsu, M., et al. (2002), NCEP dynamical seasonal forecast system 2000, *Bull. Am. Meteorol. Soc.*, *83*, 1019–1037, doi:10.1175/1520-0477(2002)083<1019:NDSFS>2.3.CO;2.
- Kistler, R., et al. (2001), The NCEP-NCAR 50-year reanalysis: Monthly mean CD-ROM and documentation, *Bull. Am. Meteorol. Soc.*, *82*, 247–267, doi:10.1175/1520-0477(2001)082<0247:TNNYRM>2.3.CO;2.
- Kuroda, Y. (2008a), Role of the stratosphere on the predictability of the medium-range weather forecast: A case study of winter 2003–2004, *Geophys. Res. Lett.*, *35*, L19701, doi:10.1029/2008GL034902.
- Kuroda, Y. (2008b), Effect of stratospheric sudden warming and vortex intensification on the tropospheric climate, *J. Geophys. Res.*, *113*, D15110, doi:10.1029/2007JD009550.
- Kuroda, Y., and K. Kodera (2001), Variability of the polar-night jet in the Northern and Southern hemispheres, *J. Geophys. Res.*, *106*, 20,703–20,713, doi:10.1029/2001JD900226.
- Kuroda, Y., and K. Kodera (2004), Role of the polar-night jet oscillation on the formation of the Arctic oscillation in the Northern Hemisphere winter, *J. Geophys. Res.*, *109*, D11112, doi:10.1029/2003JD004123.

- Lorenz, E. N. (1963), Deterministic nonperiodic flow, *J. Atmos. Sci.*, *20*, 130–141, doi:10.1175/1520-0469(1963)020<0130:DNF>2.0.CO;2.
- Mizuta, R., et al. (2006), 20-km-mesh global simulation using JMA-GSM model—Mean climate states, *J. Meteorol. Soc. Jpn.*, *84*, 165–185, doi:10.2151/jmsj.84.165.
- Thompson, D. W. J., and J. M. Wallace (1998), The Arctic oscillation signature in the wintertime geopotential height and temperature fields, *Geophys. Res. Lett.*, *25*, 1297–1300, doi:10.1029/98GL00950.
-
- Y. Kuroda, Meteorological Research Institute, 1-1 Nagamine, Tsukuba, Ibaraki 305-0052, Japan. (kuroda@mri-jma.go.jp)